All optical wavelength broadcast based on simultaneous Type I QPM broadband SFG and SHG in MgO:PPLN

Mingjun Gong,[1] Yuping Chen,[1,2] Feng Lu,[1] and Xianfeng Chen[1,3]

[1]*Department of Physics, the State Key Laboratory on Fiber Optics Local Area Communication Networks and Advanced Optical Communication Systems, Shanghai Jiao Tong University, 800 Dongchuan Road, Shanghai 200240, China*

[2]*E-mail: ypchen@sjtu.edu.cn*

[3]*E-mail: xfchen@sjtu.edu.cn*

Received March 29, 2010; revised July 6, 2010; accepted July 8, 2010; posted July 19, 2010 (Doc. ID 126112); published August 4, 2010

We experimentally demonstrate wavelength broadcast based on simultaneous Type I quasi-phase-matched (QPM) broadband sum-frequency generation (SFG) and second-harmonic generation (SHG) in 5 mol.% MgO-doped periodically poled lithium niobate (MgO:PPLN). One signal has been synchronously converted into seven different wavelengths using two pumps at a 1.5 μm band via quadratic cascaded nonlinear wavelength conversion. By selecting different pump regions, i.e., selecting different cascaded $\chi^{(2)}:\chi^{(2)}$ interactions, the flexible wavelength conversions with shifting from one signal to single, double, and triple channels were also demonstrated.

OCIS codes: 190.2620, 190.4360, 230.7405, 230.1150, 130.3730.

As for future wavelength division multiplexed (WDM) optical networks, wavelength conversion (WC) is a crucial function for dynamic channels routing and reallocation [1]. With data transmission growing rapidly, wavelength broadcast that can replicate a signal into several channels is urgently demanded in high-speed and large-capacity optical networks. All optical WC and WDM broadcasts based on semiconductor optical amplifiers were demonstrated [2,3], but these suffer from low conversion speed [4]. As an alternative scheme, wavelength conversion based on quasi-phase-matched (QPM) nonlinear optical interactions in periodically poled lithium niobate (PPLN) has attracted much interest for ultrafast response speed, transparency to signal format, and bit rates. Efficient WC using QPM difference-frequency generation (DFG) and cascaded second-order nonlinearity ($\chi^{(2)}:\chi^{(2)}$) in PPLN have been demonstrated [5,6]. Multiple channel WCs were realized in designed structures with the aim of wavelength broadcast [7–9]. However, the discrete and fixed QPM wavelengths with narrow second-harmonic generation (SHG) bandwidth (Type 0 QPM) limit their flexibility and tunability once the structures are engineered. Broadband wavelength broadcast based on cascaded $\chi^{(2)}:\chi^{(2)}$ in PPLN will be the most promising candidate for all optical networks [9,10].

In this Letter, we report wavelength broadcast by cascaded $\chi^{(2)}:\chi^{(2)}$ WC at a 1.5 μm band in MgO:PPLN, based on simultaneous Type I QPM broadband sum-frequency generation (SFG) and SHG. A signal being broadcast to seven wavelengths using two pumps was demonstrated experimentally. Choosing different pump wavelengths for flexible WC with shifting from one signal to single, double, and triple channels was performed. Advantages of this wavelength broadcast, such as variable destination channels and output channel number, constructible, and mobile broadband, are believed to be attractive in the optical communication system.

In our experiments, we proposed utilizing cascaded SHG/DFG and SFG/DFG (cSHG/DFG and cSFG/DFG) to realize wavelength broadcast, where the 1.5 μm band cw lights were upconverted to a 0.77 μm band by SFG or SHG, and then the idler lights were generated by DFG. The experimental setup is similar to previous work (see [11]), but another pump is added. Polarization controllers are implemented to ensure that the 1.5 μm band lights are ordinary waves in z-cut MgO:PPLN for Type I interactions. The size of MgO:PPLN is 20 mm $\times$ 10 mm $\times$ 0.5 mm, and its poling period is 20.4 μm, which satisfies broadband QPM conditions for both SHG and SFG at the 1.5 μm band [6,10]. To generate new frequency waves, two pumps ($\lambda_{p1} = 1544.72$ nm and $\lambda_{p2} = 1547.91$ nm) and one signal ($\lambda_s = 1546.68$ nm) were coupled and amplified by a C-band erbium-doped fiber amplifier (EDFA). We found the signal was converted to seven wavelengths, as shown in Fig. 1. When only one pump was presented, the signal was shifted to two channels (c1 and c5 with pump1; c3 and c6 with pump2) via cSHG/DFG. While two pumps were presented, another three new channels (c2, c4, and c7) yielded via

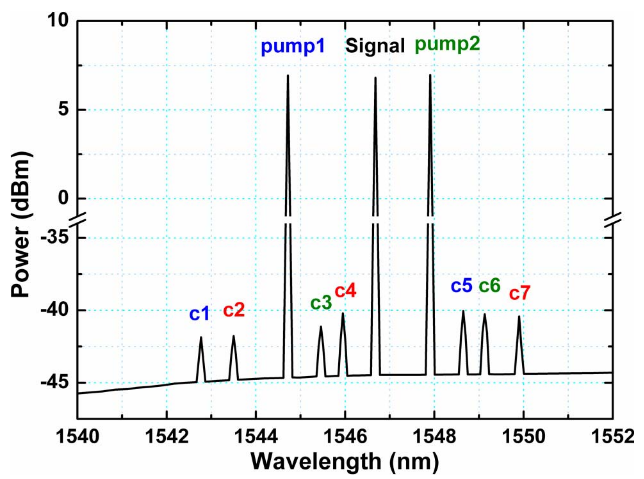

Fig. 1. (Color online) Measured signal ($\lambda_s = 1546.68$ nm) broadcast spectrum using two pumps ($\lambda_{p1} = 1544.72$ nm and $\lambda_{p2} = 1547.91$ nm) based on cascaded $\chi^{(2)}:\chi^{(2)}$ interactions.

0146-9592/10/162672-03$15.00/0

cSFG/DFG, because two input waves can generate a sum-frequency wave, which then interacts with the other one (one of the three input 1.5 μm band lights including two pumps and one signal) by DFG to yield a new wave. So the signal was broadcast to seven channels owing to simultaneous cSHG/DFG and cSFG/DFG.

In this MgO:PPLN, wavelength broadcast is accomplished based on broadband QPM SFG and SHG. First, at the optimal temperature of 38.2 °C, we obtained a 21 nm SHG broadband around the central QPM wavelength 1549.80 nm. To obtain broadband SHG, we employed Type I QPM using d_{31} (about 1/6 of d_{33} with Type 0 QPM), which decreased the efficiency ($\sim$1/36) and brought about power penalty. With incident pump power 300 mW, the normalized second-harmonic (SH) efficiency is about 1%/W. Then two pumps (named pump λ_p and pump0 λ_{p0}) were employed to illustrate broadband SFG and SHG. We fixed λ_{p0} at 1560.64 nm, which was located at the edge of SHG broadband, so the second-harmonic wave of pump0 was weak, while λ_p was tuned from 1528 to 1561 nm. Figure 2 shows the generated sum-frequency (SF of λ_p and λ_{p0}) and second-harmonic (SH of λ_p) waves varying with λ_p. Diamonds and circles represent the experimental SF and SH waves, while the dashed and solid curves are calculated SFG and SHG bandwidth curves from Eq. (1) [10,12] at 36.3 °C, which is slightly different from the operation temperature 38.2 °C because of the Sellmeier equation uncertainty of MgO:PPLN [13]:

$$\eta \propto \mathrm{sinc}^2(\Delta k_i L/2), \qquad (1)$$

where L is the length of MgO:PPLN, $\Delta k_i (i = \mathrm{SH}, \mathrm{SF})$ is the wave-vector mismatch including the QPM grating vector $2\pi/\Lambda$ (Λ is the poling period of MgO:PPLN), and

$$\Delta k_{\mathrm{SH}} = 2\pi n_{\mathrm{SH}}/\lambda_{\mathrm{SH}} - 4\pi n_p/\lambda_p - 2\pi/\Lambda, \qquad (2)$$

$$\Delta k_{\mathrm{SF}} = 2\pi n_{\mathrm{SF}}/\lambda_{\mathrm{SF}} - 2\pi n_p/\lambda_p - 2\pi n_{p0}/\lambda_{p0} - 2\pi/\lambda. \qquad (3)$$

Here, n_i $(i = p, p0, \mathrm{SH}, \mathrm{SF})$ is the refractive index at pumps and SH and SF wavelengths, respectively, and

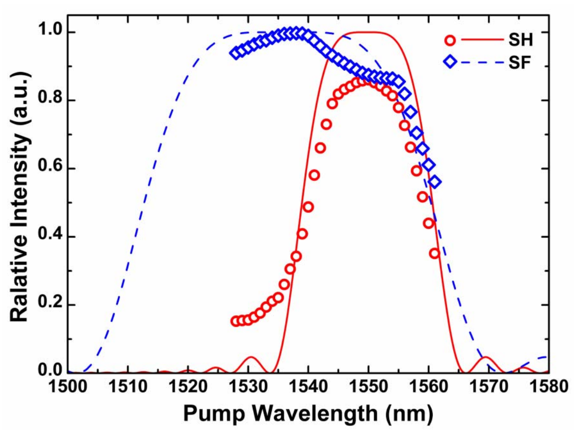

Fig. 2. (Color online) Type I QPM broadband SFG and SHG with pump0 fixed at 1560.64 nm. The the dashed and solid curves indicate calculated SFG and SHG bandwidth at 36.3 °C, while the diamonds and circles are the experimental SF and SH waves at 38.2 °C, respectively.

$1/\lambda_{\mathrm{SH}} = 2/\lambda_p$ and $1/\lambda_{\mathrm{SF}} = 1/\lambda_p + 1/\lambda_{p0}$. With λ_p tuning within the overlapping range of broadband SFG and SHG, simultaneous SF and SH waves were generated; with λ_p tuning outside the overlapping range, SFG occurred sharply and the SH wave was weak. We can see that the theoretical results basically agree with the available experimental data, with one difference—that the expected SFG bandwidth is broader than that shown in Fig. 3, which is limited by the gain bandwidth of C-band EDFA.

By selecting a different pump region, we performed shifting from one signal to single, double, and triple channels. In this demonstration, the signal just participates in

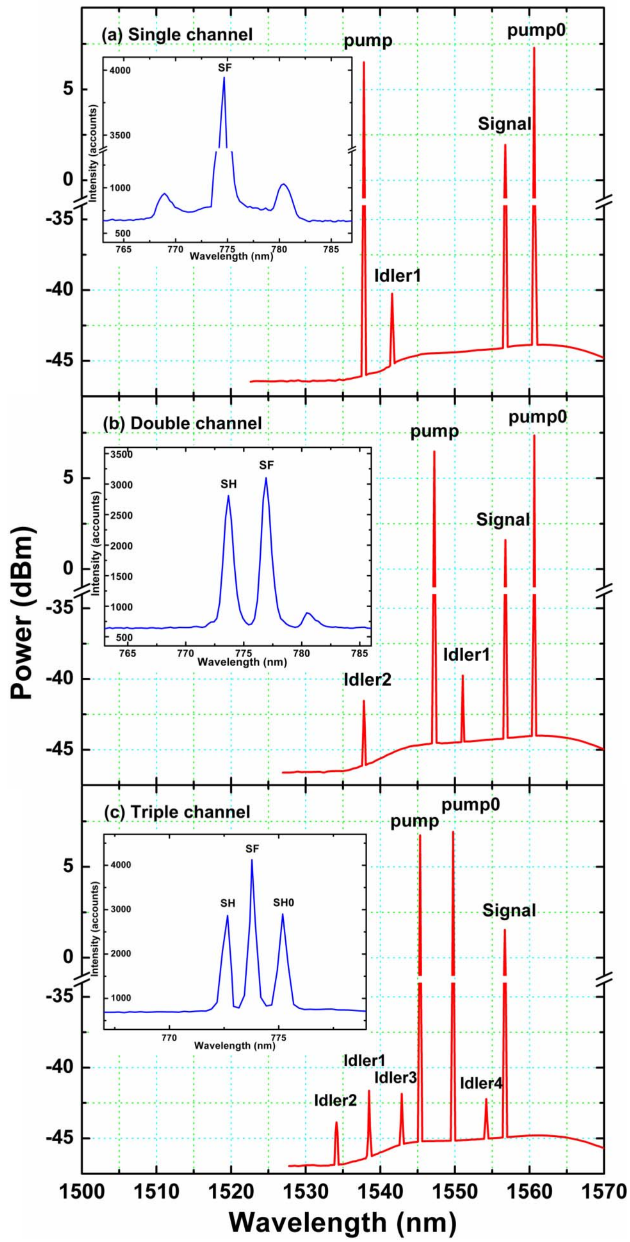

Fig. 3. (Color online) Measured $\chi^{(2)}:\chi^{(2)}$ wavelength conversion spectrums with $\lambda_s = 1556.77$ nm. (a) Single channel ($\lambda_{p0} = 1560.64$ nm and $\lambda_p = 1537.82$ nm), (b) double channel ($\lambda_{p0} = 1560.64$ nm and $\lambda_p = 1547.23$ nm), (c) triple channel ($\lambda_{p0} = 1549.75$ nm and $\lambda_p = 1545.33$ nm). The insets illustrate the SF and SH waves.

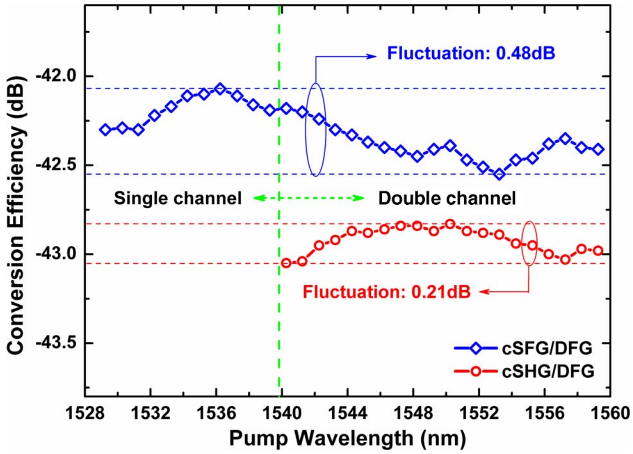

Fig. 4. (Color online) Wavelength conversion efficiency versus pump wavelength via cSFG/DFG and cSHG/DFG.

the latter DFG process and was set at $\lambda_s = 1556.77$ nm. Figure 3 shows the measured WC spectra with different pumps. In Figs. 3(a) and 3(b), pump0 was fixed at 1560.64 nm, while λ_p varied from a nonoverlapping region to an overlapping region and the signal was converted to a single channel (idler1: $\omega_{i1} = \omega_{p0} + \omega_p - \omega_s$) and a double channel (idler1: $\omega_{i1} = \omega_{p0} + \omega_p - \omega_s$ and idler2: $\omega_{i2} = 2\omega_p - \omega_s$). The insets illustrate the SF and SH waves. When both pumps were located in the SHG broadband, SF and SH waves were generated simultaneously. As shown in Fig. 3(c), the signal was converted to a triple channel (idler1: $\omega_{i1} = \omega_{p0} + \omega_p - \omega_s$; idler2: $\omega_{i2} = 2\omega_p - \omega_s$; and idler3: $\omega_{i3} = 2\omega_{p0} - \omega_s$). The idler4 ($\omega_{i4} = 2\omega_{p0} - \omega_p$) appeared because λ_p and λ_{p0} were close and cSHG/DFG occurred between them.

The conversion efficiency defined as $\eta = P_i/P_s$ (P_i and P_s are the output power of idlers and signal from the end of the crystal, respectively) versus pump wavelength was shown in Fig. 4, while λ_s and λ_{p0} were kept at 1556.77 and 1560.64 nm, respectively. Both pump powers were about 7 dBm, and the signal power was about 2 dBm. The small fluctuations of conversion efficiency for cSFG/DFG and cSHG/DFG ensure that each converted channel has analogous efficiency.

As [10,12,14] mention, for Type I $\chi^{(2)}$ processes, the phase-velocity mismatch can be compensated by a QPM grating period; due to a small group-velocity mismatch (GVM) between pumps, SH and SF waves and broadband SFG and SHG are expected. The phase-velocity mismatch can be compensated macroscopically by designing an appropriate poling period, whereas the GVM properties depend on the material dispersion that can be tailored microscopically with MgO doping, waveguide structure, and temperature tuning [14]. Namely, the QPM broadband can be artificially tailored and shifted to the desired operation wavelength range [12,14]. These properties are useful for effective frequency extension and distortion-free WC of ultrafast pulse [14,15].

Owing to the broadband SFG and SHG and choosing proper pump wavelengths and pump number, the signal can be shifted to desired output channels. The number of broadcast channels and the destination channels are variable. With the pump wavelength detuning and the channel number increasing, each channel has similar conversion efficiency, which would not decrease significantly. Moreover, satisfactions of phase velocity mismatch and small GVM enable efficient WC of pulse interactions for high-speed optical networks [15]. Waveguide structure fabrication in MgO:PPLN can be adopted to enhance conversion efficiency up to about –30 dB. To pursue more preferable conversion efficiency and broader bandwidth, other QPM ferroelectric materials with larger off-diagonal nonlinear optical coefficient and smaller dispersion, such as $KNbO_3$, etc., are also anticipated for wavelength broadcast [10,14].

In summary, we obtained simultaneous Type I QPM broadband SFG and SHG in MgO:PPLN at a communication band. One signal was broadcast to seven channels utilizing two pumps. By choosing a different pump region, the flexible wavelength conversion shifting the signal to single, double, and triple channels was demonstrated. Several advantages of this scheme are believed to have promising applications in all optical networks.

This work is supported by the National High Technology Research and Development Program (863) of China (2007AA01Z273), the National Natural Science Fund of China (10874120 and 60407006), and the Scientific Research Foundation for the Returned Overseas Chinese Scholars, State Education Ministry.

References

1. S. J. B. Yoo, IEEE J. Lightwave Technol. **14**, 955 (1996).
2. K. Obermann, S. Kindt, D. Breuer, and K. Petermann, IEEE J. Lightwave Technol. **16**, 78 (1998).
3. J. Pleumeekers, J. Leuthold, M. Kauer, P. G. Bernasconi, C. A. Burrus, M. Cappuzzo, E. Chen, L. Gomez, and E. Laskowski, in *Optical Fiber Communications Conference*, Vol. 70 of OSA Trends Optics Photonics, A. Sawchuk, ed. (Optical Society of America, 2002), paper ThDD4.
4. K. Gallo and G. Assanto, J. Opt. Soc. Am. B **16**, 741 (1999).
5. M. H. Chou, J. Hauden, M. A. Arbore, and M. M. Fejer, Opt. Lett. **23**, 1004 (1998).
6. C. Q. Xu and B. Chen, Opt. Lett. **29**, 292 (2004).
7. M. H. Chou, K. R. Parameswaran, M. M. Fejer, and I. Brener, Opt. Lett. **24**, 1157 (1999).
8. Y. W. Lee, F. C. Fan, Y. C. Huang, B. Y. Gu, B. Z. Dong, and M. H. Chou, Opt. Lett. **27**, 2191 (2002).
9. M. Asobe, O. Tadanaga, H. Miyazawa, Y. Nishida, and H. Suzuki, Opt. Lett. **28**, 558 (2003).
10. N. E. Yu, J. H. Ro, M. Cha, S. Kurimura, and T. Taira, Opt. Lett. **27**, 1046 (2002).
11. J. Zhang, Y. Chen, F. Lu, and X. Chen, Opt. Express **16**, 6957 (2008).
12. J. Zhang, Y. Chen, F. Lu, W. Lu, W. Dang, X. Chen, and Y. Xia, Appl. Opt. **46**, 7792 (2007).
13. D. E. Zelmon, D. L. Small, and D. Jundt, J. Opt. Soc. Am. B **14**, 3319 (1997).
14. N. E. Yu, S. Kurimura, K. Kitamura, J. H. Ro, M. Cha, S. Ashihara, T. Shimura, K. Kuroda, and T. Taira, Appl. Phys. Lett. **82**, 3388 (2003).
15. Y. Wang, J. Fonseca-Campos, C. Xu, S. Yang, E. A. Ponomarev, and X. Bao, Appl. Opt. **45**, 5391 (2006).